# Evaluation of Wavelet Filters for Image Compression

G. Sadashivappa, and K. V. S. AnandaBabu

**Abstract**—The aim of this paper to characterize a larger set of wavelet functions for implementation in a still image compression system using SPIHT algorithm. This paper discusses important features of wavelet functions and filters used in sub-band coding to convert image into wavelet coefficients in MATLAB. Image quality is measured objectively—using peak signal to noise ratio (PSNR) and its variation with bit rate (bpp). The effect of different parameters is studied on different wavelet functions. Our results provide a good reference for application—designers of wavelet based coder.

*Keywords*—Wavelet, image compression, sub band, SPIHT, PSNR.

#### I. INTRODUCTION

DATA compression techniques help in efficient data transmission, storage and utilization of hardware resources. Uncompressed multimedia requires considerable storage capacity and transmission bandwidth. Despite rapid progress in mass- storage density, processor speeds and digital communication system performance, demand for data storage capacity and data transmission bandwidth continues to outstrip the capabilities of available technologies. The recent growth of intensive digital audio, image and video (multi media) based applications, have not only sustained the compression of such signals central to signal storage and digital communication technology. Table I shows the multimedia data types and its requirements. This information clearly suggests the need of compression.

# II. IMAGE COMPRESSION SCHEMES

Image compression reduces the amount of data required to represent an image by removing redundant information. Three types of redundancies typically exist in digital images that can be exploited by compression. These are, coding redundancy that arises from the representation of the image gray levels, interpixel redundancy that exists due to high correlation between neighboring pixels, and psycho visual redundancy that is obtained based on Human perception of the image information [8]. An image compression system consists of an

encoder that exploits one or more of the above redundancies to represent the image data in a compressed manner, and a decoder that is able to reconstruct the age from the compressed data. The compression that is performed on images can either be lossless or lossy. Images compressed in a lossless manner can be reconstructed exactly without any change in the intensity values. This limits the amount of compression that can be achieved in images encoded using lossless techniques. However, many applications such as satellite image processing and certain medical and document imaging, do not tolerate any losses in their data and are frequently compressed using lossless compression methods. Lossy encoding is based on trading off the achieved compression or bit rate with the distortion of the reconstructed image. Lossy encoding for images is usually obtained using transform encoding methods. Transform domain coding is used in images to remove the redundancies by mapping the pixels into a transform domain prior to encoding. The mapping is able to represent image information containing most of the energy into a small region in the transform domain requiring only a few transform coefficients to represent. For compression, only the few significant coefficients must be encoded, while a majority of the insignificant transform coefficients can be discarded without significantly affecting the quality of the reconstructed image. An ideal transform mapping should be reversible and able to completely decor relate the transform coefficients.

TABLE I Multimedia Data

MULTIMEDIA DATA							
Multimedia	Size/duration	Bits/pixel or	Uncompressed				
data		Bits/sample	size				
Page of text	11" x 8.5"	Varying	16-32 Kbits				
		resolution					
Telephone	1 Sec	8 bps	64 Kb/sec				
quality							
speech							
Gray scale	512 x 512	8 bpp	2.1 Mb/image				
image							
Color	512 x 512	24 bpp	6.29 Mb/image				
image			_				
Medical	2048 x 2048	12 bpp	100 Mb/image				
image							
Full motion	640 x 640,10	24 bpp	2.21 Gbits				
Video	Sec						

G. Sadashivappa is Assistant Professor in the Department of Telecommunication Engineering, R. V. College of Engineering, Mysore Road, Bangalore-59, Karnataka, India (e-mail:g sadashivappa@yahoo.com).

K.V.S. Ananda Babu is the Principal of C.M.R.Institute of Technology, No.132, AECS Layout; I.T.Park Road, Bangalore -37, Karnataka, India (e-mail:anandkvs@hotmail.com).

## III. WAVELET BASED IMAGE CODING

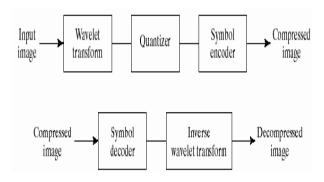


Fig. 1 Wavelet based Image Coding System

Fig. 1 shows the wavelet based coder has three basic components: a transformation, a quantizer and an encoder. Most existing high performance image coders in applications are transform based coder [1]. In the transform coder, the image pixels are converted from the spatial domain to the transform domain through a linear orthogonal or bi-orthogonal transform. A good choice of transform accomplishes a decorrelation of the pixels, while simultaneously providing a representation in which most of the energy is usually restricted to a few (relatively large) coefficients. This is the key to achieve an efficient coding (i.e., high compression ratio). Indeed, since most of the energy rests in a few large transform coefficients, we may adopt entropy coding schemes, e.g., runlevel coding or bit plane coding schemes, that easily locate those coefficients and encodes them. Because the transform coefficients are highly decorrelated, the subsequent quantizer and entropy coder can ignore the correlation among the transform coefficients, and model them as independent random variables.

The zerotree concept [1], provided an efficient and embedded representation of quantized wavelet coefficients and lead to an image compression method, the embedded zerotree wavelet (EZW) coding. A zero tree is used to represent a particular group of wavelet coefficients across different wavelet sub bands that have insignificant values. The zero tree approach exploits the multiresolution nature of the wavelet decomposition and has lead to several other low complexity and extremely efficient image compression schemes. One of the more popular methods based on similar principles of the zerotree is the SPIHT [3], by Said and Pearlman, which improves upon the EZW with better management of the zerotrees. The SPIHT method is discussed in more detail in the section-V. The JPEG2000 image coding standard [7, 18] also achieves its superior performance due to the wavelet transform-based embedded block coding with optimal truncation (EBCOT) scheme. These encoding schemes described above are fast, are efficient, have low complexity, and provide high quality images at extremely low bit rates, making them suitable for image transmission across channels with bandwidth constraints. The progressive nature of these schemes, however, results in the encoded data being highly susceptible to bit errors, causing severe distortions to

the resulting image. Steps must be therefore taken to protect the encoded bit stream from being affected by various bit errors and losses.

## IV. IMAGE QUALITY MEASURE

The image quality can be evaluated objectively and subjectively. Objective methods are based on computable distortion measures [8, 12]. Standard objective measures of image quality are Mean Square Error (MSE) and Peak Signal-to-Noise Ratio (PSNR) which are defined as

$$_{MSE} = \frac{1}{MN} \sum_{y=1}^{M} \sum_{x=1}^{N} \left[ I\left(x,y\right) - I'\left(x,y\right) \right]^{2} \tag{1}$$

And

$$PSNR = 20 * log10 (255 / sqrt(MSE))$$
 (2)

Where I(x,y) is the original image, I'(x,y) is the approximated version (which is actually the decompressed image) and M,N are the dimensions of the images. MSE and PSNR are the most common methods for measuring the quality of compressed images, despite the fact that they are not adequate as perceptually meaningful measures of image quality. Equation (2) is for commonly used 8bpp images.

In image compression systems, the truly definitive measure of image quality is perceptual quality. The distortion is specified by mean opinion score (MOS) or by picture quality scale (PQS). MOS is perception based subjective evaluation where as PQS is perception based objective evaluation. PQS methodology uses some of the properties of HVS relevant to global image impairments, such as random errors, and emphasizes the perceptual importance of structured and localized errors. PQS is constructed by regressions with MOS, which is 5-level grading scale developed for subjective evaluation. (5-imperceptible, 4 – perceptible, but not annoying, 3 – slightly annoying, 2 – annoying, 1 – very annoying). The compression efficiency is defined by the parameter compression ratio, CR and is given by,

For example, if actual bpp = 8 and reduced bpp = 0.5 then CR = 16:1. If original data =  $512 \times 512 \times 8 = 1.497152$  Bits and compressed data = 1.497152 Bits then CR = 1000:1.

## V. THEORETICAL CONCEPTS

## A. Wavelet Theory

Wavelet and Wavelet technique have recently generated much interest, both in applied areas as well as in mathematical ones. The class of Wavelet techniques is not really precisely defined and it keeps changing. Hence, it is virtually impossible to give a precise definition of wavelet that incorporates all different aspects. It is equally hard to write a comprehensive overview of wavelets. In this paper, we restricted to focus on wavelets which satisfy the important properties for image compression like orthogonal and orthonormal (db N and bior Nd, Nr class of wavelets).

Wavelet theory involves representing general functions interims of simpler, fixed building blocks at different scales and positions. This has been found to be a useful approach in several different areas, like sub band coding, quadrature mirror filters, pyramid schemes, etc. Further, wavelets permit multiresolutin analysis with the following properties: orthogonality, compact support, rational coefficients, symmetry, smoothness, number of vanishing moments and analytic expressions. Fig. 4 shows structural properties of db9 and bior6.8 as a specific case. These are the low pass and high pass filters used in the wavelet decomposition of image. In experimentation, we Considered 512 reconstruct.bmp image which is available in MAT LAB to test different wavelet filters at different levels of decomposition. By considering global thresholding, dbN filters tested for retained energy in % and number of zeros in % where as bior Nd, Nr filters are tested for normal coefficients recovery in% and number of zeros in %. Table-II, TableIII (A) and III (B) gives the results, it is observed that for better compression the level of decomposition should be grater than 3. The type and order of filter depends on symmetry and vanishing moments.

# B. Wavelet Transform

Discrete Wavelet transform requires two sets of related functions called scaling function and wavelet function. Most of the scaling and wavelet functions are fractal in nature and iterative methods are required to see its shape. Most good and modern image compression schemes are based on the wavelet transform. Wavelets have been identified as basis functions or building blocks that can be used to produce all possible functions. They can also quickly decorrelate data [19,20], which can lead to a more compact representation than the original data. In addition, wavelets have the special feature that all the wavelet functions can be constructed from a single mother wavelet w(t), which is effectively a small wave. The other wavelet functions, wij(t) are obtained from the mother wavelet by translation and compression or dilation as shown below.

Where i and j represent the scaling (compression or dilation) and the translation parameters, respectively. The compression and translation allow the wavelet functions to represent signals in multiple levels of time-frequency resolutions. The multiresolution representation of wavelets along with their

orthogonal properties makes them attractive for representation of various functions. The wavelet transform is implemented in the discrete time domain by the discrete wavelet transform (DWT). The DWT can be implemented by passing the signal through a combination of low pass and high pass filters and down sampling by a factor of two to obtain a single level of decomposition. Multiple levels of the wavelet transform are performed by repeating the filtering and down sampling operation on low pass branch outputs.

The 1-D wavelet transform can be extended to a twodimensional wavelet transform using separable filters. The 2-D transform is performed by applying a 1-D transform along the rows and then along the columns. An n-level 2-D wavelet decomposition of a signal is shown in Figure 2. In the figure, ho(x) and go(x) represent the lowpass and highpass filter responses, respectively. The filter outputs at level n are given by an, hn, vn, and dn, respectively. The lowpass filter output from the previous level serves as the input for the next level of decomposition. The use of biorthogonal wavelets has been found to be the most suitable for obtaining image wavelet transforms for compression applications. The biorthogonal filters have linear phase and symmetric properties that are useful in avoiding boundary artifacts in images [8]. One of the most popular set of biorthogonal filters are the Daubechies' 9/7 analysis and synthesis filters, used quite commonly for image compression applications. The 2-D wavelet transform, when applied to images, provides decorrelation and yields a spatial-frequency distribution of the image.

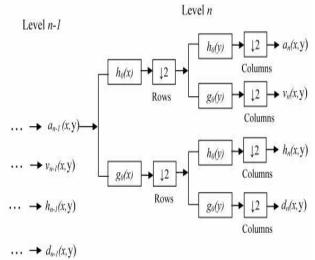


Fig. 2 n-level wavelet decomposition of a 2-D input

a  $(x,\ y)$  - approximation coefficient ,  $v(\ x,\ y\ )$  - vertical coefficient

h ( x ,y ) – horizontal coefficient , d ( x, y ) – diagonal coefficient

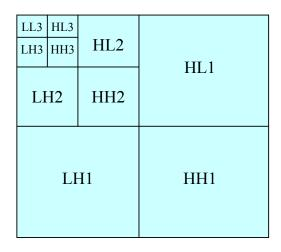
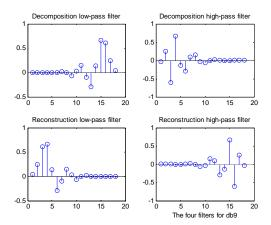


Fig. 3 3-Level dyadic wavelet pyramid

In general, most of the energy in the image tends to be concentrated in the low frequency regions with the detail sub bands containing the edge information. Furthermore the energy in the high frequency bands is concentrated into a relatively small number of coefficients. The probability distribution of wavelet coefficients in the high frequency sub bands has been shown to have a generalized Gaussian-like distribution with a high concentration of near zero valued coefficients [2, 10]. The spatial-frequency distribution of images due to the wavelet transform leads to an effective grouping of coefficients for compression. Fig. 3 gives the 3level dyadic wavelet pyramid representation of an image. Where suffix 1 indicates first level 2 is second level and 3 is third level of decomposition. For biorthogonal property we consider only DbN and Bior Nd, Nr family of wavelets in our simulation. To show the symmetry property of the filters, only db9 and bior6.8 wavelet filter are shown in Fig. 4.



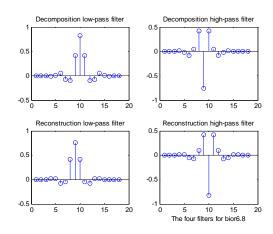


Fig. 4 Four Wavelet filters for db9 and bior6.8

TABLE II
dbN Wavelet Filter Response (Energy Compaction)

	Retained energy in %	Number of zeros in %		
L	1 2 3	1 2 3		
	4 5	4 5		
WF				
Db1	99.88 99.42 98.30	75.00 93.75 98.30		
	98.85 98.91	98.35 98.90		
Db2	99.99 99.89 99.61	75.00 93.64 98.36		
	99.28 99.37	99.28 99.38		
Db3	100 99.95 99.74	75.00 93.60 98.30		
	99.09 99.20	99.08 99.20		
Db4	100 99.95 99.72	75.00 93.50 98.21		
	99.21 99.34	99.21 99.34		
Db5	100 99.97 99.07	75.00 93.46 98.18		
	99.04 99.18	99.04 99.18		
Db6	100 99.99 99.58	75.00 93.36 98.10		
	99.09 99.22	99.08 99.22		
Db7	100 99.98 <b>99.34</b>	75.00 93.32 <b>98.02</b>		
	98.96 <b>99.15</b>	98.96 <b>99.15</b>		
Db8	100 99.98 <b>99.45</b>	75.00 93.22 <b>97.95</b>		
	98.94 <b>99.10</b>	98.96 <b>99.10</b>		
Db9	100 99.98 <b>99.55</b>	75.00 93.18 <b>97.92</b>		
	98.93 <b>99.06</b>	98.93 <b>99.08</b>		
Db1	100 99.98 <b>99.31</b>	75.00 93.08 <b>97.84</b>		
0	98.85 <b>99.00</b>	98.86 <b>99.00</b>		

TABLE III (A)
BIOR Nd,Nr WAVELET FILTER RESPONSE (ENERGY RECONSTRUCTION )
NORMAL COEFFICIENTS RECOVERY IN %

L       1       2       3       4       5         Wavelet       Bior1.1       99.88       99.42       98.30       98.85       98.91         Bior1.3       99.88       99.44       99.17       98.78       98.94         Bior1.5       99.88       99.33       98.57       98.97       99.15         Bior2.2       100       99.92       99.72       99.21       99.34         Bior2.4       100       99.97       99.07       99.04       99.18         Bior2.6       100       99.90       99.58       99.09       99.22         Bior2.8       100       99.95       99.34       98.96       99.15         Bior3.1       100       99.97       99.45       98.94       99.10         Bior3.3       100       99.97       99.55       98.93       99.06         Bior3.7       100       99.96       99.31       98.85       99.00         Bior3.9       100       99.96       98.94       98.61       98.74         Bior4.4       100       99.98 <b>99.24</b> 99.20 <b>99.35</b>	
Bior1.1         99.88         99.42         98.30         98.85         98.91           Bior1.3         99.88         99.44         99.17         98.78         98.94           Bior1.5         99.88         99.33         98.57         98.97         99.15           Bior2.2         100         99.92         99.72         99.21         99.34           Bior2.4         100         99.97         99.07         99.04         99.18           Bior2.6         100         99.90         99.58         99.09         99.22           Bior2.8         100         99.95         99.34         98.96         99.15           Bior3.1         100         99.97         99.45         98.94         99.10           Bior3.3         100         99.97         99.55         98.93         99.06           Bior3.5         100         99.96         99.31         98.85         99.00           Bior3.7         100         99.97         98.97         98.89         98.98           Bior3.9         100         99.96         98.94         98.61         98.74	
Bior1.1         99.88         99.42         98.30         98.85         98.91           Bior1.3         99.88         99.44         99.17         98.78         98.94           Bior1.5         99.88         99.33         98.57         98.97         99.15           Bior2.2         100         99.92         99.72         99.21         99.34           Bior2.4         100         99.97         99.07         99.04         99.18           Bior2.6         100         99.90         99.58         99.09         99.22           Bior2.8         100         99.95         99.34         98.96         99.15           Bior3.1         100         99.97         99.45         98.94         99.10           Bior3.3         100         99.97         99.55         98.93         99.06           Bior3.5         100         99.96         99.31         98.85         99.00           Bior3.7         100         99.97         98.97         98.89         98.98           Bior3.9         100         99.96         98.94         98.61         98.74	
Bior1.3         99.88         99.44         99.17         98.78         98.94           Bior1.5         99.88         99.33         98.57         98.97         99.15           Bior2.2         100         99.92         99.72         99.21         99.34           Bior2.4         100         99.97         99.07         99.04         99.18           Bior2.6         100         99.90         99.58         99.09         99.22           Bior2.8         100         99.95         99.34         98.96         99.15           Bior3.1         100         99.97         99.45         98.94         99.10           Bior3.3         100         99.97         99.55         98.93         99.06           Bior3.5         100         99.96         99.31         98.85         99.00           Bior3.7         100         99.97         98.97         98.89         98.98           Bior3.9         100         99.96         98.94         98.61         98.74	
Bior1.5         99.88         99.33         98.57         98.97         99.15           Bior2.2         100         99.92         99.72         99.21         99.34           Bior2.4         100         99.97         99.07         99.04         99.18           Bior2.6         100         99.90         99.58         99.09         99.22           Bior2.8         100         99.95         99.34         98.96         99.15           Bior3.1         100         99.97         99.45         98.94         99.10           Bior3.3         100         99.97         99.55         98.93         99.06           Bior3.5         100         99.96         99.31         98.85         99.00           Bior3.7         100         99.97         98.97         98.89         98.98           Bior3.9         100         99.96         98.94         98.61         98.74	
Bior2.2         100         99.92         99.72         99.21         99.34           Bior2.4         100         99.97         99.07         99.04         99.18           Bior2.6         100         99.90         99.58         99.09         99.22           Bior2.8         100         99.95         99.34         98.96         99.15           Bior3.1         100         99.97         99.45         98.94         99.10           Bior3.3         100         99.97         99.55         98.93         99.06           Bior3.5         100         99.96         99.31         98.85         99.00           Bior3.7         100         99.97         98.97         98.89         98.98           Bior3.9         100         99.96         98.94         98.61         98.74	
Bior2.4         100         99.97         99.07         99.04         99.18           Bior2.6         100         99.90         99.58         99.09         99.22           Bior2.8         100         99.95         99.34         98.96         99.15           Bior3.1         100         99.97         99.45         98.94         99.10           Bior3.3         100         99.97         99.55         98.93         99.06           Bior3.5         100         99.96         99.31         98.85         99.00           Bior3.7         100         99.97         98.97         98.89         98.98           Bior3.9         100         99.96         98.94         98.61         98.74	
Bior2.6         100         99.90         99.58         99.09         99.22           Bior2.8         100         99.95         99.34         98.96         99.15           Bior3.1         100         99.97         99.45         98.94         99.10           Bior3.3         100         99.97         99.55         98.93         99.06           Bior3.5         100         99.96         99.31         98.85         99.00           Bior3.7         100         99.97         98.97         98.89         98.98           Bior3.9         100         99.96         98.94         98.61         98.74	
Bior2.8         100         99.95         99.34         98.96         99.15           Bior3.1         100         99.97         99.45         98.94         99.10           Bior3.3         100         99.97         99.55         98.93         99.06           Bior3.5         100         99.96         99.31         98.85         99.00           Bior3.7         100         99.97         98.97         98.89         98.98           Bior3.9         100         99.96         98.94         98.61         98.74	
Bior3.1         100         99.97         99.45         98.94         99.10           Bior3.3         100         99.97         99.55         98.93         99.06           Bior3.5         100         99.96         99.31         98.85         99.00           Bior3.7         100         99.97         98.97         98.89         98.98           Bior3.9         100         99.96         98.94         98.61         98.74	
Bior3.3     100     99.97     99.55     98.93     99.06       Bior3.5     100     99.96     99.31     98.85     99.00       Bior3.7     100     99.97     98.97     98.89     98.98       Bior3.9     100     99.96     98.94     98.61     98.74	
Bior3.5     100     99.96     99.31     98.85     99.00       Bior3.7     100     99.97     98.97     98.89     98.98       Bior3.9     100     99.96     98.94     98.61     98.74	
Bior3.7 100 99.97 98.97 98.89 98.98 Bior3.9 100 99.96 98.94 98.61 98.74	
Bior3.9 100 99.96 98.94 98.61 98.74	
<b>Bior4.4</b> 100 99.98 <b>99.24</b> 99.20 <b>99.35</b>	
<b>Bior5.5</b> 100 99.98 <b>99.40</b> 99.23 <b>99.41</b>	
<b>Bior6.8</b> 100 99.99 <b>99.61</b> 99.95 <b>99.17</b>	

TABLE III(B)
BIOR Nd,Nr Wavelet Filter Response (Energy Reconstruction)
Number of Zeros in %( biorNd,Nr )

L	1	2	3	4	5
Wavelet					
Bior1.1	75.00	93.75	98.30	98.85	98.90
Bior1.3	75.00	93.64	98.17	98.78	98.95
Bior1.5	75.00	93.46	98.18	98.97	99.20
Bior2.2	75.00	93.50	98.21	99.21	99.34
Bior2.4	75.00	93.46	98.18	99.04	99.18
Bior2.6	75.00	93.36	98.10	99.08	99.22
Bior2.8	75.00	93.32	98.02	98.96	99.15
Bior3.1	75.00	93.22	97.95	98.96	99.10
Bior3.3	75.00	93.18	97.92	98.93	99.08
Bior3.5	75.00	93.08	97.84	98.86	99.00
Bior3.7	75.00	93.22	97.95	98.79	98.98
Bior3.9	75.00	93.08	97.84	98.61	98.74
Bior4.4	75.00	93.46	98.18	99.20	99.35
Bior5.5	75.00	93.36	98.10	99.23	99.41
Bior6.8	75.00	93.18	97.92	98.95	99.17

Table III (A) and (B) gives the energy compaction and reconstruction properties of orthogonal filters db and bior category. It is observed that with respect to dbN category, for L=3, the energy retained in % and number of zeros in % are not equal. This suggests there is a scope for compression, whereas for L=5, both the parameters are equal and it is optimized level of decomposition. In the case of biorNd,Nr,

same logic holds good. For L=3, normal coefficients recovery in % and number of zeros in % are not equal, it is equal for L=5. Hence maximum value for L is 5, beyond which no improvement in compression and further increases delay in operation (MOP will increase).[12]

Table IV and Fig. 5 gives the variation of PSNR with respect to level of decomposition L by keeping CR at 10:1. This will suggest selecting the optimum value of L

TABLE IV
EFFECT OF LEVEL OF DECOMPOSITION (L), CR=10:1
PSNR VALUES FOR DIFFERENT WAVELET FILTERS

WF	Db7	Db9	Bior2	Bior	Sym5	Coif5
L			2	4. 4		
2	16.91	16.92	17.88	16.73	16.92	16.93
3	33.10	31.00	33.15	33.21	33.15	33.32
4	37.46	37.38	37.38	37.88	37.70	37.82
5	38.24	38.16	38.13	38.48	38.28	38.37
6	38.35	38.25	38.22	38.65	39.03	38.52

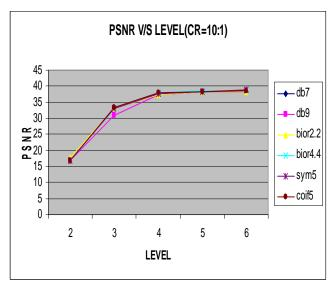


Fig. 5 Graph for PSNR v/s LEVEL ( L) of decomposition

# C. Set-Partitioning in Hierarchical Trees (SPIHT)

The SPIHT algorithm, developed by Said and Pearlman in 1996 [3], is a fast and efficient image compression algorithm that works by testing ordered wavelet coefficients for significance in a decreasing bit plane order, and quantizing only the significant coefficients. The high coding efficiency obtained by this algorithm is due to a group testing of the coefficients that belong to a wavelet tree. Group testing is advantageous because of the inter-band correlation that exists between the coefficients belonging to a tree. The SPIHT uses the fundamental idea of zero-tree coding from the EZW but is able to obtain a more efficient and better compression performance in most cases without having to use an arithmetic encoder.

The SPIHT algorithm groups the wavelet coefficients and trees into sets based on their significance information. The

encoding algorithm consists of two main stages, sorting and refinement. In the sorting stage, the threshold for significance is set as 2n, where n is the bit level, and its initial value is determined by the number of bits required to represent the wavelet coefficient with the maximum absolute value. Significance for trees is obtained by checking all the member detail coefficients. Approximation coefficients are tested as individual entries. The initial listing that determines the order in which significance tests are done is predetermined for both the approximation coefficients as well as the trees. The algorithm searches each tree, and partitions the tree into one of three lists: 1) the list of significant pixels (LSP) containing the coordinates of pixels found to be significant at the current threshold; 2) the list of insignificant pixels (LIP), with pixels that are not significant at the current threshold; and 3) the list of insignificant sets (LIS), which contain information about trees that have all the constituent entries to be insignificant at the current threshold. If a coefficient or a tree is found to be insignificant, a "0" bit is sent to the output bit stream and the corresponding coordinates are moved to the LIP or LIS respectively, for subsequent testing at a lower bit level. When a coefficient is found to be significant, a "1" bit and a sign bit are sent out and its coordinate is moved to the LSP. If an LIS member is found to be significant, a "1" bit is sent out and the tree is partitioned into its offspring and descendants of offspring. The offspring are moved to the end of the LIP and subsequently tested for significance at the same bit level. The offspring are also moved to the LIS as the roots of their corresponding descendant sets that will be subsequently tested for significance at the same bit level. The bit level is successively lowered, and the precision of every member of the LSP found significant at the previous bit level is enhanced by sending the next bit from the binary representation of their values. This operation is called the refinement stage of the algorithm.

The refinement allows for successive approximation quantization of the significant coefficients. When the bit level is decremented, the sorting pass is applied in the same manner as before to the remaining LIP and LIS constituents. The encoding process terminates when the desired bit rate or quality level is reached. In the decoder, the output of the significance tests are received, and therefore the same lists (LIP, LIS, and the LSP) can be built, as in the encoder. As input bits are read from the bit stream, the decoder reconstructs the magnitude and sign bits of LSP members as seen by the encoder. The coefficients of the final LIP and LIS sets, corresponding to those coefficients that are insignificant with respect to the last bit level, are set to zero. Thus a scalar quantizer with a dead zone is effectively implemented. The synchronized ordering of information for interpretation at the decoder, along with the refinement process, leads to a progressive coding scheme, where even a truncated bit stream can be decoded to get a lower rate image. However, it is the synchronized ordering of list information that makes images compressed with SPIHT very susceptible to data loss.

Using the SPIHT algorithm developed by Jing Tian, to achieve higher compression ratio L is taken as 5 and different wavelet filters have been tested for different bit rates. Table gives the simulated results. The test image is Lena 512 x 512,

8bpp gray scale. The error metric used to compare different filters is PSNR.

TABLE V (A)
PSNR PERFORMANCE OF DIFFERENT FILTERS

I = 5 I ENA GRAY IMAGE 512 x 512 - SRPP

С	Врр	Db1	db7	Db9	Bior2.	Bior4.
R		(haar)			2	4
8	1	37.37	39.57	39.51	39.14	39.75
16	0.5	33.29	36.02	35.87	35.74	36.35
32	0.25	29.83	32.40	32.29	32.30	32.79
64	0.125	26.95	28.83	28.78	28.90	29.26
12	0.062	24.05	25.57	25.48	25.63	25.61
8	5					
25	0.031	20.84	21.75	21.62	22.18	21.63
6	25					

TABLE V (B)
PSNR PERFORMANCE OF DIFFERENT FILTERS
L=5. LENA GRAY IMAGE 512 x 512. 8BPP.

CR	Врр	Coif1	Coif5	Sym1	Sym5
8	1	38.92	39.72	37.37	39.60
16	0.5	35.10	36.28	33.29	36.12
32	0.25	31.49	32.70	29.83	32.64
64	0.125	28.26	29.06	26.95	29.11
128	0.0625	25.03	25.78	24.05	25.69
256	0.03125	21.26	21.91	20.84	21.78

## VI. CONCLUSION

Table V gives the simulation results for Lena 512 x 512 gray image for SPIHT algorithm [13]. With respect to rate-distortion response, the minimum value of PSNR assumed to be 30 db, and then level of decomposition should be more than 3. And if L is beyond 4 not much improvement in PSNR. For CR of 32:1, it is observed that db7, bior4.4, coif5 and sym5 perform better. Further it is required to study other characteristics of wavelet filters for optimization.

## ACKNOWLEDGMENT

The Authors like to thank Dr.S.C.Sharma, Principal, and Prof. K.N.RajaRao, Vice-Principal & Head, Department of Telecommunication Engineering, R. V. College of Engineering, for their support and encouragement.

## REFERENCES

- J.M.Shapiro, "Embedded image coding using Zero trees of wavelet coefficients, IEEE Trans. Signal Processing, Vol 41, pp 3445-3462, Dec 1993.
- [2] Vetterli .M and Kovacevic .J, "Wavelets and sub band coding", Englewood cliffs, NJ, Prentice Hall 1995.
- [3] Amir.Said and W.A.Pearlman, "A new fast and efficient image codec based on set partitioning in hierarchical trees" IEEE Trans Circuits Syst. Video Technol, Vol 6, pp 243-250, June 1996.
- [4] Charles D. Creusere. A new method of robust image compression based on the embedded zerotree wavelet algorithm. IEEE Trans. on Image Processing, 6(10):1436–1442, October 1997.

## International Journal of Electrical, Electronic and Communication Sciences

ISSN: 2517-9438 Vol:3, No:3, 2009

- [5] K.Sayood, "Introduction to Data Compression", 2nd edition, Academic Press, Morgan Kaufman Publishers, 2000.
- [6] David Solomon, "Data Compression The Complete Reference", 3rd edition, Springer.
- [7] David Taubman. High performance scalable image compression with EBCOT. IEEE Trans. on Image Processing, 9:1158–1170, July 2000.
- [8] Sonja Grgic, Mislov Grgic and Branka Zorko-cihlar, "Performance Analysis of Image Compression Using Wavelets" IEEE Trans on Industrial Electronics, Vol 48, No 3, June 2001.
- [9] Rafael C. Gonzalez and Richard E. Woods. Digital Image Processing. Pearson Education, Englewood Cliffs, 2002.
- [10] Raghuveer Rao and Ajit. B. Bopadikar, "Introduction to Theory and Applications-Wavelet Transforms", Pearson Education Asia, New Delhi, 2004.
- [11] James. E.Fowler and Beatrice Pesuet-Popescu, "An Overview on Wavelets in Source Coding, Communication, and Networks," EURSIP Journal on Image and Video Processing, Vol 2007.
- [12] G.Sadashivappa, K.V.S. AnandaBabu, "erformance analysis of Image Coding Using Wavelets" IJCSNS International Journal of Computer Science and Network Security, Oct.2008
- [13] website: http://ipl.rpi.edu/SPIHT
- [14] R.Sudhakar, Ms.R.Karthiga, S.Jayaraman-Image Compression using Coding of Wavelet Coefficients- A Survey , GVIP, www.icgst.com
- [15] Coding of Still Pictures ISO/IEC JTC1/SC29/WG1 (ITU-T SG8)
- [16] A. Bovik, Ed, Hand Book Of Image and Video Processing, SanDiego. CA, Academic, 2000
- [17] Bernd Girod, Robert Gray, Image and Video Coding, IEEE Signal Processing Magazine, M arch 1998
- [18] A. Skodras, C. Christopoulos, and T.Ebrahimi, The JPEG 2000 Still Image Compression Standard IEEE Signal Processing Magazine 2001
- [19] G.M.Davis, A. Nosratinia, Wavelet based image coding: An Overview Applied and computational control, Signals and circuits, Vol 1, No1, 1998
- [20] M. Antonini, M. Barland, P.Mathica, I.Daubechies, Image coding Using Wavelet Transform, IEEE Trans Image Processing, vol 5, No 1, pp 205-220, 1992.
- G. Sadashivappa, received the BE degree in Electronics Engineering from Bangalore University in 1984 and M.Tech degree in Industrial Electronics from NIT-K, Mangalore University in1991. During 1984-1989 he worked as Lecturer in AIT Chickmagalore, JMIT Chitradurga and Engineer trainee in Kirloskar Electric Co Ltd Mysore. Since 1992, is working in R.V.College of Engineering. He is pursuing his Doctoral program at VTU Belgaum. His research interests are Image & Video Coding, Signal Processing and fiber optic networks.
- **K.V.S.** Ananda Babu graduated from IIT Madras in 1969, obtained M.Tech from IIT Delhi in 1983. He obtained doctorate from Osmania University, Osmania in 2000. His research interests are Adaptive Signal Processing, Image & Video Coding and Channel Coding. He has 31 years of research experience in DRDO labs. Currently working as Principal CMRIT, Bangalore.